DESIGN OF AN RF-GRIDDED GUN FOR A HIGH-EFFICIENCY TRISTRON

A. S. Thakur†, W. L. Millar, I. Syratchev, European Organization for Nuclear Research, Geneva, Switzerland
G. Burt, Z. Un Nisa, Lancaster University, Lancaster, United Kingdom

Abstract

The RF gridded gun is a key component of the RF power sources chosen for the FCC-ee tristron. It enables the generation of bunched electron beams via the application of an RF voltage across the cathode-grid gap. The tristron allows a compact tube architecture and provides high RF power production efficiency. The emitted, grid intercepted, and transmitted beam currents are governed by the applied RF grid voltage and DC cathode voltage, providing additional degrees of freedom for controlling the bunch formation. For continuous wave tristron operation at an RF power level of 0.5 MW in the UHF band, particular attention must be paid to several critical design aspects, including beam grid interception, beam optics design, thermomechanical effects, and stress. These factors strongly influence the operational stability, device lifetime, and overall performance. The current status of the RF gridded gun design for the tristron is reported.

INTRODUCTION

Gridded vacuum electron devices, such as the Inductive Output Tube (IOT) [1], are well known for their high efficiency in high-power RF applications. However, their efficiency is fundamentally limited by the quality of electron bunching. To overcome this limitation, the tristron concept was proposed as an extended IOT configuration incorporating an additional idler cavity to improve bunching and achieve significantly higher RF conversion efficiency [2]. Therefore, the multibeam (MB) tristron has emerged recently as a promising RF power source for FCC-ee [3]. In this work, the conceptual design and numerical investigation of a gridded gun for an MB tristron are presented, with emphasis on beam formation, beam-grid interception, and current modulation.

GRIDDED GUN NUMERICAL STUDIES

The MB tristron is currently selected as the baseline 400 MHz, 0.5 MW continuous wave RF power source for the FCC-ee. It offers a high operational efficiency, compact and cost-efficient solution [4]. The gridded gun is one of the most critical components of the tristron. We designed this device starting with common recommendations for the grid cathode spacing 0.3 mm and the grid's wire cross-section 0.15 mm × 0.15 mm. The hexagonal (HEX) grid topology (Fig. 1, right) was selected based on a comparative analysis with other grid configurations, where the HEX grid appeared to be superior in terms of heat evacuation. Contrary to the spherical cathodes with electrostatic focusing (beam area compression) normally used in conventional IOTs [1, 5], we selected a flat cathode-grid assembly without beam compression. This choice simplifies the beam optics (Fig. 1, left) as the cathode itself is embedded in the constant magnetic field of 0.08 T provided by the external solenoid.

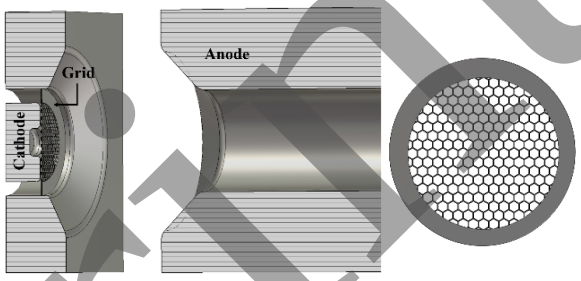

Figure 1: The gridded gun setup (left) and the hexagonal grid (right) used in the CST simulations.

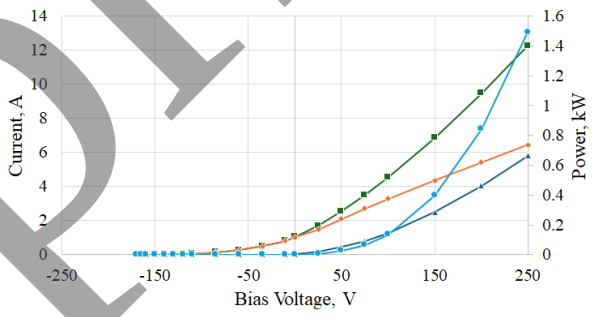

Figure 2: Emitted (rectangles), grid-intercepted (triangles), and transmitted (diamonds) currents, together with the power intercepted on grid (circles) versus bias voltage.

To avoid current emission from the cathode when the input RF signal is inhibited, the grid is operated at DC bias with respect to the cathode voltage [5]. The optimum value of this bias voltage depends on the ratio between the cathode-grid gap and the grid-anode gap lengths, the cathode voltage, as well as the grid opacity to the electric field.

In the proposed gridded gun configuration, a 46 kV voltage is applied to the cathode-anode gap. Using the CST 3D beam tracking (TRK) software, we simulated DC parameters in the system like emitted current, current intercepted on the grid, power intercepted on the grid, and transmitted current as functions of the grid bias voltage (Fig. 2). Here a -165 V DC voltage should be applied to block the current emission. It shall be noted that, following the standard approach applied in CST user community, the cathode in simulations is assigned to a ground potential and anode is set to a positive potential.

In an approximation of very short cathode-grid gap, the bunched beam current envelopes and transient intercepted

†aditya.singh.thakur@cern.ch

beam power can be calculated using interpolated data from TRK simulations shown in Fig. 2:

$$V_{\text{grid}} = V_{\text{bias}} + |V_{\text{rf}}|sin(\omega t) \quad (1)$$

$$I, P\big(V_{\text{grid}}\big) = I, P\big(V_{\text{bias}} + V_{\text{rf}}sin(\omega t)\big). \quad (2)$$

Here, V_{grid} is an instantaneous grid potential, as a superposition of an RF voltage, V_{rf}, and a DC bias voltage, V_{bias}. The variables I and P are the resulting bunched currents and beam power intercepted on the grid. In these calculations we set the bias voltage amplitude equal to its blocking value. By changing the RF voltages amplitude we now can generate bunches with the required average transmitted current. For the FCC-ee MB tristron design the avegare transmitted current is 1.07 A. The current profiles of these bunches and the transient intercepted beam power envelope calculated using the TRK + analytical (TRK_A) approach are shown in Fig. 3. To reach the desired value of the average transmitted current, an RF voltage of amplitude 305 V is applied at the grid.

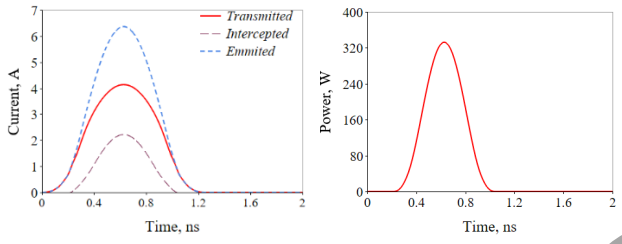

Figure 3: Bunch current profiles (left) and transient intercepted beam power (right) envelopes calculated using TRK_A. The average transmitted current is 1.07 A with an average intercepted power of 57.2 W at the grid.

The bunch length and shape information is one of the key parameters to optimize a tristron, as it defines the optimal penultimate cavity frequency detuning and the length of the drift section [4]. However, the simplified bunch shape characterization (Eqs. 1 and 2) does not include the transient group delay in a cathode-grid gap in the presence of the space charge and an external magnetic field. To obtain a more accurate analysis of the bunch generation from the gun, we used the CST 3D PIC solver.

Unfortunately, we cannot apply the space-charge limited current emission in the CST PIC simulations, which was applied in the CST TRK 3D simulations. We instead adopted a special scenario called Programmed Emmison (PE). At every given time interval, for the known amplitude and sign of the gap voltage, the emitted current value is calculated applying Eqs. 1 and 2. Such an emission current profile is generated in CST PIC with a dedicated Python script (Fig. 4). The simulation run time, using a server with two GPUs, was about 30 hours to complete it for 2500 emission sites on the cathode. In contrast, achieving a converged value for the current intercepted on the grid in TRK simulations requires an order of magnitude higher number of emission sites; however, the simulation time required to generate the dataset shown in Fig. 2 is only 3 hours.

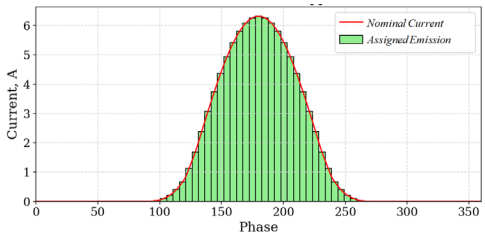

Figure 4: Discrete current emission profile generated through a Python script and assigned to the CST PIC simulation.

The results of PE PIC simulations are shown in Fig. 5, where the transmitted current pulse shape (red curve) is clearly deformed compared to the analytical pulse shape (red curve in Fig. 3). Howevere, the average current is almost identical with calculated TRK_A (Fig. 3) and PE PIC (Fig. 5). We can also observe a burst of current returning to the cathode (blue curve in Fig. 5). These particles were emitted near the end of the positive RF cycle but were unable to pass through the grid before the grid voltage reversed polarity. However, the largest difference (35 %) was observed when measuring the average beam power intercepted on the grid (Fig. 5).

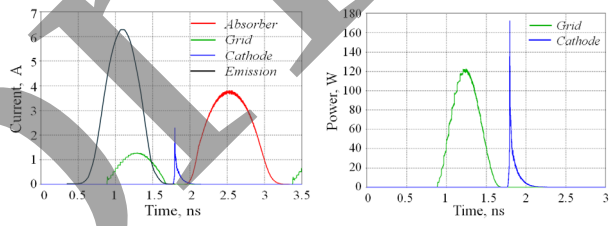

Figure 5: Bunch current profiles (left) and transient intercepted beam power (right) envelopes calculated using PE PIC. The average transmitted current is 1.05 A, with an average intercepted power of 38.5 W at the grid.

This inconsistency in the grid-intercepted beam power simulated by the two methods seems to be rather large. The major problems we faced in PE PIC is a limited number of particles used in simulations to reach saturated results and the artificial emission protocol. To solve these problems, we firstly employed the concept of the mini cathode (Fig. 6). This is a very compact arrangement with 7 kV high voltage applied to the short (10 mm) DC gap provides the same blocking biased voltage as in the big cathode, whilst beam currents and intercepted beam power are simply scaled as a ratio of the emission surfaces (factor 0.09). In this configuration we have used up to 10^4 emission sites on the cathode surface, which is equivalent to 1.12×10^5 in a full-size cathode.

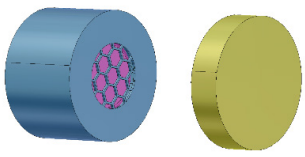

Figure 6: An isometric view of the mini-cathode topology.

Secondly, instead of using PE PIC, we decided to employ another option available in CST PIC - Field Emission (FE) protocol, which connects the surface electric field on

the cathode and emitted current density on the surface through [6]

$$J = AE^2 exp\left(-\frac{B}{E}\right). \quad (3)$$

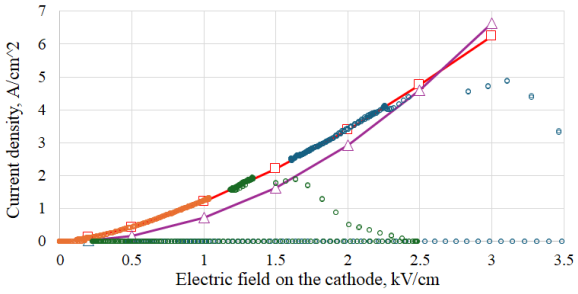

Figure 7: Current density versus electric field on the cathode surface. TRK raw data (circles) for 0 V (orange), 75 V (green) and 150 V (blue) bias voltages, space-charge limited law fit (squares) and field emission fit (triangles).

In general FE is not identical to the space charge limited emission, where the current density is proportional to $E^{1.5}$. However, by finding the appropriate values of the free parameters A and B in Eq. 3, one can generate an approximate fit between the two within the relevant parameters range. In TRK simulations, we have performed the surface current emission calibration by measuring current density over entire cathode surface for different values of the grid bias voltage. It allowed to map the current density to the cathode surface electric field including the electric field due to space-charge. This data is shown as circles in Fig. 7. The noise in the simulated data points is a numerical artefact. As expected from TRK simulations, this trend follows the space charge limited emission law (squares in Fig. 7). The free parameters in FE were fitted to generate current emission curve close enough to the measured TRK data: A=7.5×10^{-7} and B=6×10^3 (Fig. 7, triangles). Fitting criterion was to get the best agreement at a higher end of the current density.

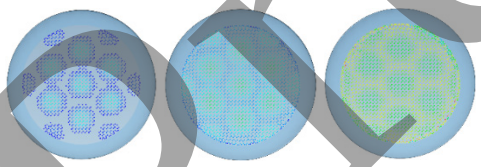

Figure 8: Snapshots of particles emission from the cathode surface at 0.2 ns (left), 0.4 ns (center), and 0.6 ns (right).

Finally, CST FE PIC simulations were carried out with an RF modulation of 305 V and a fixed bias voltage of - 165 V. As an illustration, snapshots of the particle charge distribution on the cathode surface at different moments in time are shown in Fig. 8. In this figure, current island buildup process, a well-known phenomenon in the gridded guns [4], is clearly visible. The current pulses envelope and beam power interception on the grid simulated by three different methods are compared in Fig. 9.

In terms of the average values, FE PIC and TRK_A reached a very good agreement. Thus, it is recommended as an efficient approach to optimise gridded guns. Comparing FE PIC and PE PIC, the current envelopes, along with their average values, are very similar for the transmitted pulses. However, PE PIC shows low beam power and current interception on the grid and much larger current burst returned to the cathode. Obviously, the PE PIC algorithm does not obey the actual emission processes, like current island buildup. However, it remains as a valid and computer resources efficient method to calculate the transmitted bunch distribution used for the FCC-ee MB tristron simulations with bunched beam (Fig. 10). Ultimately, FE PIC provides most accurate results, but it is presently impractical to simulate the full gridded gun topology due to the excessive computational effort (a week) to complete the simulations with available computing resources in the common scientific laboratory or university.

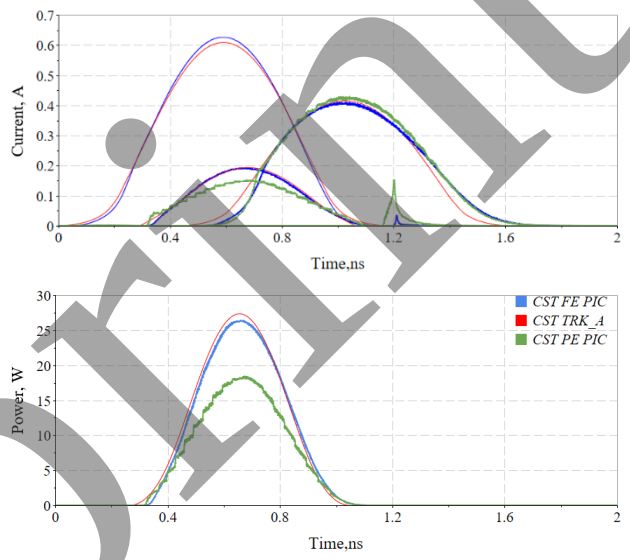

Figure 9: Current pulses in the system (top) and intercepted beam power (bottom). Results for FE PIC (blue), TRK_A (red), and PE PIC (green) methods are shown.

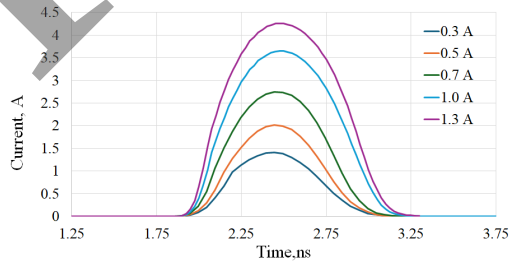

Figure 10: 400 MHz current pulses with different average current simulated using PE PIC.

CONCLUSION

The tristron RF circuit design requires precise knowledge of the bunch generated in the actual gun environment. We have developed and benchmarked different methods to perform accurate simulations of gridded guns using the commercial software CST Microwave Studio. We concluded that the TRK_A is an optimal choice for an accurate gridded gun design and the PE PIC could be used as a bunch generation technique. The developed approach was applied to generate a bunched beam in the gridded gun and export results into tristron CST PIC simulations of the RF circuit with beam.

REFERENCES

[1] A. Haeff, “An ultra-high-frequency power amplifier of novel design”, Electronics 12, no. 2, 1939, pp. 30-32.

[2] A.D. Sushkov and V.K. Fedyaev, “Electrons bunching simulations in triode-klystron (tristron)”, Izvestiya Vuzov, Radio-electronics, Vol. 10, No11, pp. 1033, 1969. [In Russian].

[3] M. Benedict *et al*.,“Future Circular Collider Feasibility Study Report Volume 2: Accelerators, technical infrastructure and safety”, CERN-FCC-ACC-2025-0004, CERN, Geneva, Switzerland, Mar. 2025. doi:10.17181/CERN.EBAY.7W4X

[4] I. Syratchev *et al.,* “The tristron, a new paradigm in high-efficiency RF power generation”, presented at the 17th International Particle Accelerator Conf. (IPAC’26), Deauville, France, May 2026, this conference.

[5] R. G. Carter, “Simple model of an inductive output tube,” in 2009 IEEE International Vacuum Electronics Conference, Ed., Apr. 2009, pp. 427–428. doi:10.1109/ivelec.2009.5193438

[6] A. S. Gilmour Jr., “Microwave Tubes”, Norwood, MA, USA: Artech House, 1986.